STRUCTURAL CHEMISTRY
ISSN 2053-2296

Weaving a 2D net of hydrogen and halogen bonds: cocrystal of a pyrazolium bromide with tetrafluorodiiodobenzene

Steven van Terwingen, Ben Ebel, Ruimin Wang and Ulli Englert*

Institute of Inorganic Chemistry, RWTH Aachen University, Landoltweg 1, 52074 Aachen, Germany. *Correspondence e-mail: ullrich.englert@ac.rwth-aachen.de

Received 23 November 2021
Accepted 2 May 2022

Edited by S. Moggach, The University of Western Australia, Australia

Keywords: crystal engineering; halogen bonds; hydrogen bonds; QTAIM; electron density.

CCDC references: 2169820; 2169819; 2169818

Supporting information: this article has supporting information at journals.iucr.org/c

Hydrohalides of Lewis bases may act as halogen bond (XB) acceptors and combine two directional interactions, namely, hydrogen bonds (HB) and XBs in the same solid. 3-(1,3,5-Trimethyl-1*H*-pyrazol-4-yl)acetylacetone ($C_{11}H_{16}N_2O_2$, HacacMePz) was protonated with H*X* (*X* = Cl or Br) to afford the hydrohalides, $C_{11}H_{17}N_2O_2^+\cdot X^-$ or H_2acacMePz$^+\cdot X^-$ (**1**, *X* = Cl; **2**, *X* = Br). Hydrohalides **1** and **2** are isomorphous and adopt a classical dipole packing. Consistent with the observation for most β-diketones, the enol form with an intramolecular HB is observed. Additional noteworthy interactions are HBs of the protonated pyrazolium towards the X^- anion at donor–acceptor distances of 2.9671 (17) Å for **1** and 3.159 (4) Å for **2**. Cocrystallization of hydrobromide **2** with the XB donor tetrafluorodiiodobenzene (TFDIB) leads to the adduct $C_{11}H_{17}N_2O_2^+\cdot Br^-\cdot 0.5C_6F_4I_2\cdot H_2O$ or $(H_2$acacMePz$^+\cdot Br^-)_2\cdot(H_2O)_2\cdot$TFDIB (**3**), in which the XB donor TFDIB is situated on a crystallographic centre of inversion. Classical HBs link organic cations, water molecules and Br^- anions into chains along [010]. Almost orthogonal to this interaction, XBs with Br$\cdots$I = 3.2956 (4) Å connect neighbouring chains along [102] into two-dimensional sheets in the $(10\bar{2})$ plane. Assisted by their negative charge, halide anions represent particularly good nucleophiles towards XB donors.

1. Introduction

In recent decades, the field of crystal engineering has evolved rapidly (Desiraju, 2010; Aakeröy *et al.*, 2010). The ability to tailor solids for specific applications, such as gas separation (Wu *et al.*, 2018; Gao *et al.*, 2020) and storage (Müller *et al.*, 2017), sensing (Lustig *et al.*, 2017), catalysis (Rimer *et al.*, 2018) and other areas (Blagden *et al.*, 2007; Zhang *et al.*, 2018), has contributed to this triumph.

Our group has used heterobifunctional molecules such as *N*-donor functionalized acetylacetones (Kremer & Englert, 2018) as ligands for the selective construction of heterobimetallic coordination polymers. These examples rely on covalent and coordinative bonds, sometimes in combination with hydrogen bonds, *e.g.* in metal–organic frameworks like MOF-5 (Li *et al.*, 1999). In this contribution, we focus on the weaker yet also decisive combination of two essentially electrostatic and highly directional interactions, hydrogen bonds (HB) and halogen bonds (XB) (Saha *et al.*, 2005; Aakeröy *et al.*, 2013). These attractive interactions have gained increasing interest in recent years from both experimental and theoretical aspects (Costa, 2018; Cavallo *et al.*, 2016). Halogen bonds are formed between a Lewis base and a (mostly heavy) halogen. The latter exhibits an electron-deficient site opposite to its σ-bond, the so-called σ-hole (Politzer *et al.*, 2007; Clark *et al.*, 2007; Politzer *et al.*, 2017). This σ-hole is particularly

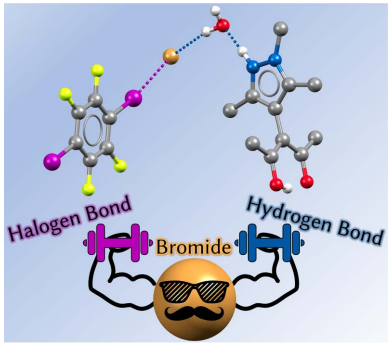

Table 1
Experimental details.

Experiments were carried out at 100 K with Mo $K\alpha$ radiation using a Bruker APEX CCD diffractometer. Absorption was corrected for by multi-scan methods (*SADABS*; Bruker, 2008). H atoms were treated by a mixture of independent and constrained refinement.

	1	**2**	**3**
Crystal data			
Chemical formula	$C_{11}H_{17}N_2O_2^+\cdot Cl^-$	$C_{11}H_{17}N_2O_2^+\cdot Br^-$	$C_{11}H_{17}N_2O_2^+\cdot Br^-\cdot 0.5C_6F_4I_2\cdot H_2O$
M_r	244.71	289.17	508.12
Crystal system, space group	Orthorhombic, *Pbca*	Orthorhombic, *Pbca*	Monoclinic, $P2_1/c$
a, b, c (Å)	8.770 (2), 11.658 (3), 23.843 (6)	8.859 (4), 12.038 (5), 23.805 (10)	12.9151 (2), 11.3061 (2), 12.5239 (2)
α, β, γ (°)	90, 90, 90	90, 90, 90	90, 90.6281 (5), 90
V (Å^3)	2437.9 (11)	2538.7 (18)	1828.62 (5)
Z	8	8	4
μ (mm^{-1})	0.30	3.23	3.97
Crystal size (mm)	0.34 × 0.17 × 0.14	0.13 × 0.06 × 0.03	0.19 × 0.15 × 0.08
Data collection			
T_{min}, T_{max}	0.619, 0.746	0.595, 0.745	0.563, 0.749
No. of measured, independent and observed [$I > 2\sigma(I)$] reflections	32185, 3104, 2482	26167, 2321, 1647	170884, 15145, 11531
R_{int}	0.088	0.096	0.091
Refinement			
$R[F^2 > 2\sigma(F^2)]$, $wR(F^2)$, S	0.042, 0.112, 1.05	0.037, 0.099, 1.04	0.042, 0.093, 1.10
No. of reflections	3104	2321	15145
No. of parameters	156	156	235
No. of restraints	0	1	5
$\Delta\rho_{max}$, $\Delta\rho_{min}$ (e Å^{-3})	0.39, −0.34	0.58, −0.58	1.19, −0.78

Computer programs: *SMART* (Bruker, 2009), *SAINT* (Bruker, 2009), *SHELXT2014* (Sheldrick, 2015*a*), *SHELXL2018* (Sheldrick, 2015*b*) and *PLATON* (Spek, 2020).

pronounced in polyfluorinated iodobenzenes, in which the polarizable iodine acts as the halogen-bond donor. Lewis bases such as halides or organic molecules with a lone-pair donor act as matching counterparts, *i.e.* XB acceptors. X-ray diffraction has provided information beyond geometry and confirmed the σ-hole model from theory: experimental charge–density studies based on high-resolution diffraction data have provided insight into the nature of strong (Bianchi *et al.*, 2003, 2004; Wang *et al.*, 2012, 2018*a*, 2019) and weak (Otte *et al.*, 2021) XBs, and even for hypervalent iodine compounds, such as Togni reagent I (Wang *et al.*, 2018*b*). The above-mentioned linkers in crystal engineering, our ditopic molecules, not only act as Lewis bases towards metal cations but can also engage in halogen bonds as nucleophiles (Merkens *et al.*, 2013) and as Brønsted bases towards mineral acids. We recently reported the cocrystal of a substituted pyrazolium chloride and 1,2,4,5-tetrafluoro-3,6-diiodobenzene (TFDIB), in which the chloride anion engages in a hydrogen and a halogen bond in an orthogonal fashion (van Terwingen *et al.*, 2021*a*). Interestingly, we found that the reported molecule does not cocrystallize with TFDIB alone, most probably due to steric hindrance around the N-donor atom. Quite obviously, a proton is much smaller than any halogen-bond donor; therefore, we exploited a hydrohalic acid to introduce this proton and a halide as a halogen-bond acceptor at the same time. The structural results were used for a single-point calculation, and the topology of the resulting electron density was analyzed by Bader's Quantum Theory of Atoms in Molecules (QTAIM) (Bader, 1990). Both hydrogen and halogen bonds are reflected in bond paths with appreciable electron density in their bond critical points (bcps). We proposed this to be prototypic for a new class of cocrystals in which hydrohalides of organic Lewis bases and halogen-bond donors co-exist in the same solid and possibly build extended structures. Further studies on our heterobifunctional molecules led to the target structure of this contribution, with a substituted pyrazolium bromide, water and TFDIB as constituents. Chemical diagrams for the pyrazolium halides and the bromide cocrystal with TFDIB are shown in Scheme 1.

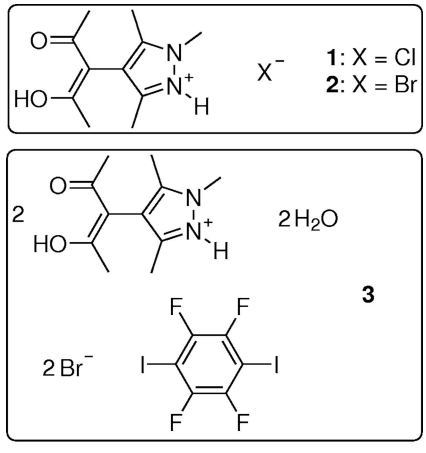

Scheme 1

2. Experimental

2.1. Materials and methods

All chemicals were used without further purification. HacacMePz was prepared as described previously (van Terwingen *et al.*, 2021*b*). Magnetic resonance spectra were measured using a Bruker Avance II Ultrashield 11 plus 400

spectrometer (400 MHz, referenced to tetramethylsilane). IR spectra were recorded with a Shimadzu IRSpirit IR spectrometer using the ATR–IR method (ATR is attenuated total reflectance). Elemental analyses were performed using a Heraeus CHNO-Rapid VarioEL. X-ray intensity data were collected with a Bruker D8 goniometer equipped with an APEX CCD area detector and an Incoatec microsource (Mo $K\alpha$ radiation, λ = 0.71073 Å, multilayer optics). Temperature was maintained using an Oxford Cryostream 700 instrument. Powder diffraction experiments were performed on flat samples at room temperature using a STOE STADI-P diffractometer with Guinier geometry (Cu $K\alpha$, λ = 1.54059 Å, Johann germanium monochromator, STOE image-plate detector IP-PSD and a 0.005° step width in 2θ).

2.2. Refinement

Crystal data, data collection and structure refinement details are summarized in Table 1. For **1** and **2**, donor H atoms were found in a difference Fourier map. Their positions were refined freely with U_{iso}(H) = 1.5U_{eq}(O,N). For **2**, a distance restraint with a value of 0.9 Å was used for atom H1. For **3**, a disordered and a nondisordered structure model were refined. For the major component, donor H atoms were found in a difference Fourier map and refined with a distance restraint. For the minor component, donor H atoms were positioned in idealized positions at a distance of 0.85 Å. For the U_{iso}(H) value of the minority N-bonded H atom in **3**, the U_{iso}(H) value of the same H atom in the major component was used and not refined. C-bonded H atoms were positioned geometrically and refined as riding, with C—H = 0.98 Å and U_{iso}(H) = 1.5U_{eq}(C).

2.3. Computational details

The single-point calculation was carried out using the program *GAUSSIAN* (Frisch *et al.*, 2016) with the MIDIX basis set (Easton *et al.*, 1996). The fragment used was slightly larger than the asymmetric unit to include contacts of symmetry-equivalent residues; this is depicted in the supporting information. The C—H, N—H and O—H distances were corrected to values consistent with results from neutron diffraction experiments (Allen & Bruno, 2010). The electron density ρ derived from the calculation was then analyzed with *AIMAll* (Keith, 2017) and *Multiwfn* (Lu & Chen, 2012), and its topology was described according to Bader's QTAIM (Bader, 1990). As suggested by Abramov (1997), the kinetic energy G and G/ρ in the bond critical point were derived. Addtionally, the local virial theorem was used to calculate the potential energy V (Espinosa *et al.*, 1998, 1999).

2.4. Synthesis and crystallization

2.4.1. HacaMePz·H*X* (*X* = Cl for 1 and Br for 2). HacacMePz (20.8 mg, 0.1 mmol) was dissolved in acetone (2 ml). Half-concentrated hydrohalic acid (HCl: 16.6 µl; HBr: 22.8 µl) was then added. Crystals formed approximately 1 h after addition of the acid and the mixture was left unperturbed for slow solvent evaporation. After approximately 80% of the solvent had evaporated, the residual solvent was removed and the sample dried for 30 min *in vacuo*. The product was obtained as rather large colourless block-shaped crystals. Phase purity could be confirmed by powder X-ray diffraction (PXRD).

Hydrochloride **1**: yield: 14.1 mg (57.6%). CHN analysis calculated (%) for $C_{11}H_{17}ClN_2O_2$: C 54.0, H 7.0, N 11.5; found: C 54.2, H 7.0, N 11.5.

Hydrobromide **2**: yield: 19.6 mg (67.8%). CHN analysis calculated (%) for $C_{11}H_{17}BrN_2O_2$: C 45.7, H 5.9, N 9.7; found: C 45.6, H 5.8, N 9.7.

2.4.2. HacacMePz·HBr·0.5TFDIB·H$_2$O (3). HacacMePz (20.8 mg, 0.1 mmol, 2 equiv.) and 1,2,4,5-tetrafluoro-3,6-diiodobenzene (TFDIB; 20.1 mg, 0.05 mmol, 1 equiv.) were each dissolved in $CHCl_3$ (2 ml). The two solutions were combined and concentrated hydrobromic acid (wt% = 48%, 11.4 µl, 0.1 mmol, 2 equiv.) was added. The mixture was left unperturbed for slow solvent evaporation at room temperature. Crystals formed eventually after three weeks. The product was obtained as a colourless crystalline solid (yield: 44.1 mg, 86.8%). Phase purity was confirmed by PXRD. CHN analysis calculated (%) for $C_{14}H_{19}BrF_2IN_2O_3$: C 33.1, H 3.8, N 5.5; found: C 34.0, H 3.7, N 5.6.

3. Results and discussion

The coordination and crystal chemistry of the heterobifunctional molecule 3-(1,3,5-trimethyl-1*H*-pyrazol-4-yl)acetylacetone (HacacMePz), which exhibits a β-diketone alongside a Lewis basic pyrazole N-donor atom, was reported recently (van Terwingen *et al.*, 2021*b*). Protonation of the pyrazole N atom is straighforward, but attempts aimed at cocrystallization invariably bear the risk of crystallizing the hydrohalide and/or the XB donor separately. We therefore first address the structures of the hydrochloride (**1**) and hydrobromide (**2**) of HacacMePz.

3.1. Crystal structures of HacacMePz·H*X* (*X* = Cl for 1 and Br for 2)

The hydrohalides are isostructural; thus, only hydrochloride **1** will be discussed in detail. We also keep track of the angle ω, which is defined as the angle between the least-squares planes

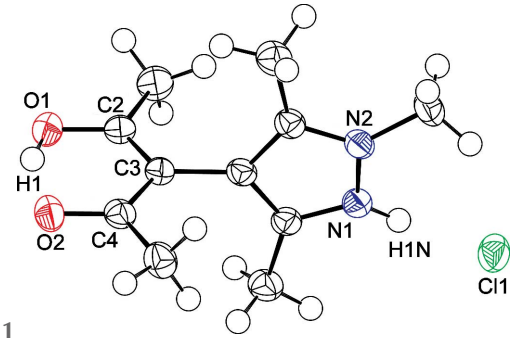

Figure 1
Displacement ellipsoid plot of the asymmetric residue of **1** (80% probability). Selected distances (Å) and angles (°): O1—C2 1.307 (2), O2—C4 1.273 (2), C2—C3 1.391 (2), C3—C4 1.429 (2), N1···Cl1 2.9671 (17) and ω 89.12 (9).

Table 2
Selected distances (Å) and angles (°) in **1** and **2**..

	O1—C2	O2—C4	N1···*X*1	ω
1	1.307 (2)	1.273 (2)	2.9671 (17)	89.12 (9)
2	1.316 (4)	1.275 (4)	3.159 (4)	85.22 (19)

of the β-diketone (atoms O1/O2/C2–C4) and the pyrazole heterocycle (N1/N2/C7–C9). In our previous work, we found this angle to be rather limited to values of approximately $90 \pm 17°$ (van Terwingen *et al.*, 2021*b*). Hydrochloride **1** crystallizes in the orthorhombic space group *Pbca*, with $Z = 8$ (Fig. 1).

As derived from the bond lengths in the acetylacetone moiety, the enol H atom is located at O1 forming an intramolecular hydrogen bond towards O2 with a distance of about 1.6 Å. A closer look at a difference Fourier map before inclusion of the enol H atom into the structure model confirms this suggestion (Fig. S1 in the supporting information); however, a second local maximum of lower electron density at atom O2 can be perceived. Tentative refinement of a structure model with a disordered enol H atom revealed a majority occupation at O1 of 65 (4)%. For the sake of simplicity, we report here the nondisordered model. Positional parameters for both the enol and the pyrazolium H atoms have been freely refined. The pyrazolium H atom forms a hydrogen bond to Cl1, with H···Cl = 2.06 (2) Å. The acetylacetone and pyrazole groups are nearly orthogonal to each other, with the ω angle being approximately 90°. There are no noteworthy intermolecular contacts between the HacacMePz·HCl moieties. The closest intermolecular distances occur between a methyl H atom and Cl1, and amount to approximately 2.7 Å. The arrangement of the hydrogen-bonded ion pairs in **1** corresponds to a classical dipole packing (Fig. 2).

Comparing hydrochloride **1** to hydrobromide **2** reveals only minor differences. Both the *a* and *b* lattice parameter are larger for **2**, while *c* is slightly smaller, resulting in an overall 100 Å^3 larger unit-cell volume for **2**. The organic residues are almost superimposable, but the hydrogen bond towards the bromide anion is about 0.2 Å longer than that to the chloride

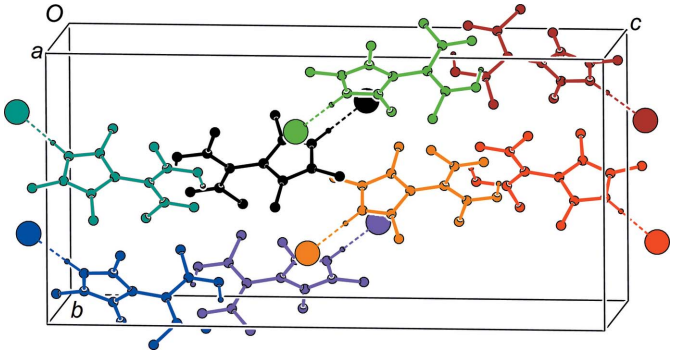

Figure 2
PLUTON plot (Spek, 2020) of the packing in **1**. Different HacacMePz·HCl moieties are depicted in different colours and reveal a classical dipole packing. H atoms not involved in short contacts have been omitted.

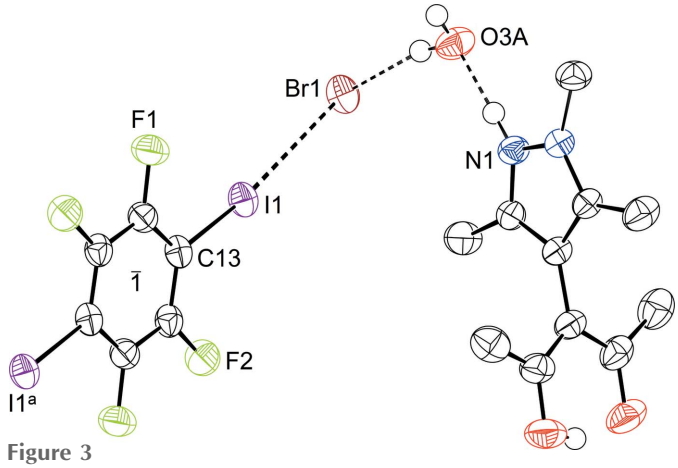

Figure 3
Displacement ellipsoid plot of **3** (80% probability, with C-bonded H atoms omitted). Selected distances (Å) and angles (°): I1···Br1 3.2957 (4), Br1···O3*A* 3.2843 (16), O3*A*···N1 2.641 (2), C13—I1···Br1 169.11 (4), I1···Br1···O3*A* 105.64 (3), Br1···O3*A*···N1 108.89 (6) and ω 84.49 (9). [Symmetry code: (*a*) $-x + 1, -y + 1, -z$.]

anion. Also, the ω angle is slightly less than in **1** at approximately 85°. No sign of enol H-atom disorder could be detected in **2**; this may be due to the unfavourable contrast of the atomic scattering factors in the hydrobromide compared to hydrochloride **1**. In this context, we also mention the pronounced difference in the linear absorption coefficients of roughly one magnitude (**1**: 0.30; **2**: 3.32 mm^{-1}). A synopsis of the important geometric differences between **1** and **2** is given in Table 2.

3.2. Crystal structure of HacacMePz·HBr·0.5TFDIB·H_2O (3)

As mentioned previously, the target cocrystallization and crystallization of the used reactants always compete and, thus, are also dependent on the solvent used. This competition is not only limited to the reactants (Aakeröy *et al.*, 2013);

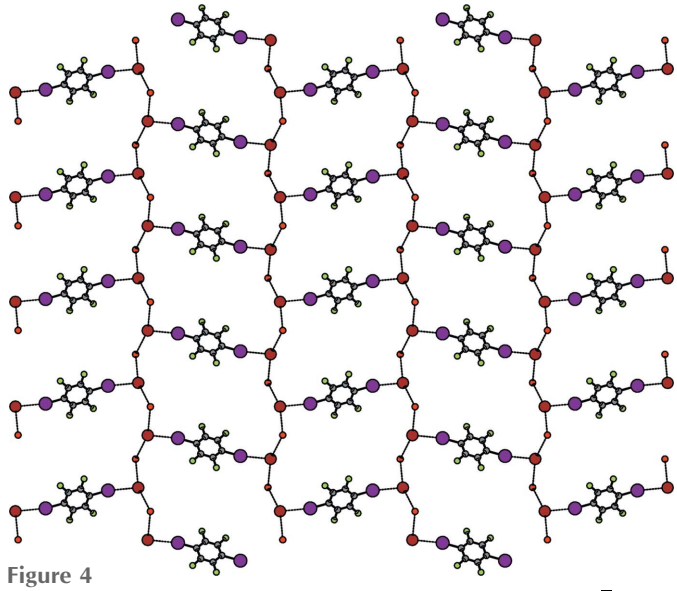

Figure 4
PLUTON plot (Spek, 2020) of the view perpendicular to the (10$\bar{2}$) plane onto the 2D net in **3** (HacacMePz and H atoms have been omitted).

Robertson *et al.* (2017) have shown that hydrogen and halogen bonds also compete, and the obtained cocrystal is highly reliant on solvent polarity. We were able to cocrystallize the hydrobromide of HacacMePz with half an equivalent of TFDIB and one solvent water molecule, and to determine its crystal structure to a high resolution of 1.00 Å^{-1}. The compound HacacMePz·HBr·0.5TFDIB·H_2O (**3**) crystallizes in the monoclinic space group $P2_1/c$ with Z = 4; a displacement ellipsoid plot is shown in Fig. 3.

Hydrohalide **3** features a hydrogen bond from the pyrazolium H atom towards the cocrystallized water molecule. The water molecule forms hydrogen bonds towards Br1 and its symmetry equivalent Br1^b [symmetry code: (b) $-x+2, y-\frac{1}{2}, -z+\frac{1}{2}$] with both its H atoms. For Br1 itself, a close contact to I1 in a rather orthogonal fashion regarding O3*A* can be observed: it accepts the σ-hole from I1 and forms a halogen bond. The TFDIB molecule is located on a centre of inversion on Wyckoff position 2*d*. A minor coupled disorder of the *N*-methyl group at N2 of HacacMePz combined with the proton at N1 and cocrystallized water molecule O3 will be discussed later.

Expanding the hydrogen-bonded contacts reveals that Br1 accepts two hydrogen bonds from symmetry-equivalent water molecules O3*A*, resulting in a one-dimensional (1D) chain with the graph-set symbol $C_2^1(4)$ (Etter, 1991) propagating along [010]. These 1D strands are connected through halogen bonds involving Br1 with the TFDIB molecules, forming a 2D net along the $(10\bar{2})$ plane with meshes formed by 14 vertices. No match for this net could be found in the Reticular Chemistry Structure Resource (RCSR; O'Keeffe *et al.*, 2008), but if the bromide anions are perceived as three-connected nodes and all other residues as linkers, the topology corresponds to a honeycomb net (**hcb**; Fig. 4).

After refinement of the structure model, closer inspection of a difference Fourier map revealed two local density maxima in close proximity to the *N*-methyl group (1.79 e$^-$) and the protonated pyrazole N1 atom (1.21 e$^-$), respectively. The first residual maximum is located at a distance of 1.498 (3) Å from N1 and the second at 2.631 (3) Å from N2. As these distances closely resemble an N—C single bond and an N—H···O hydrogen bond, we concluded that the *N*-methyl group is disordered; this disorder is coupled with split positions for the hydrogen-bonded water molecule. The site occupancy refined to 91.1 (4)% for the major component. For the minor water molecule, hydrogen bonds towards two symmetry-equivalent Br1 atoms can be found. They are, however, longer than in the major component [3.2667 (16) and 3.2843 (16) Å *versus* 3.318 (15) and 3.406 (15) Å], which may contribute to the very different occupancies of approximately 10:1 for the mutually exclusive sites. While at the rather high resolution of 1.00 Å^{-1}, the disorder is the most significant residual electron density, truncating the data to $2\theta_{max}$ = 50.3°, higher residuals around Br1 become the most prominent feature of a difference Fourier analysis. Nevertheless, the disorder is apparent also at standard resolution. All geometry data and agreement factors discussed in this article refer to the model described above, which includes the minor disorder. An alternative structure model which does not take atom sites of minor occupancy into account is available in the supporting information.

3.3. Results from a database search

A search in the Cambridge Structural Database (CSD; Groom *et al.*, 2016) for similar interactions (see supporting information for details) leads to about 200 hits. Analysis of the data shows that the distances and angles for the contacts around the halide in **3** are in the expected range (Fig. 5). Limiting the search to fluorinated iodobenzenes reduces the number of matching structures to 12, none of which shows a similar motif to **3**. The closest resemblence is found in OHOVAJ and OHOVIR (Abate *et al.*, 2009), in which the halogen bonds form a 1D chain which is expanded by amine hydrogen bonds to a 2D net. In our opinion, these results do not necessarily imply that such interactions are uncommon; they rather suggest that they have been rarely investigated.

3.4. Electron-density considerations

The Hirshfeld surface (Spackman & Jayatilaka, 2009) mapped with the distance-sensitive d_{norm} criterion reveals close contacts about bromide anion Br1 (Fig. 6).

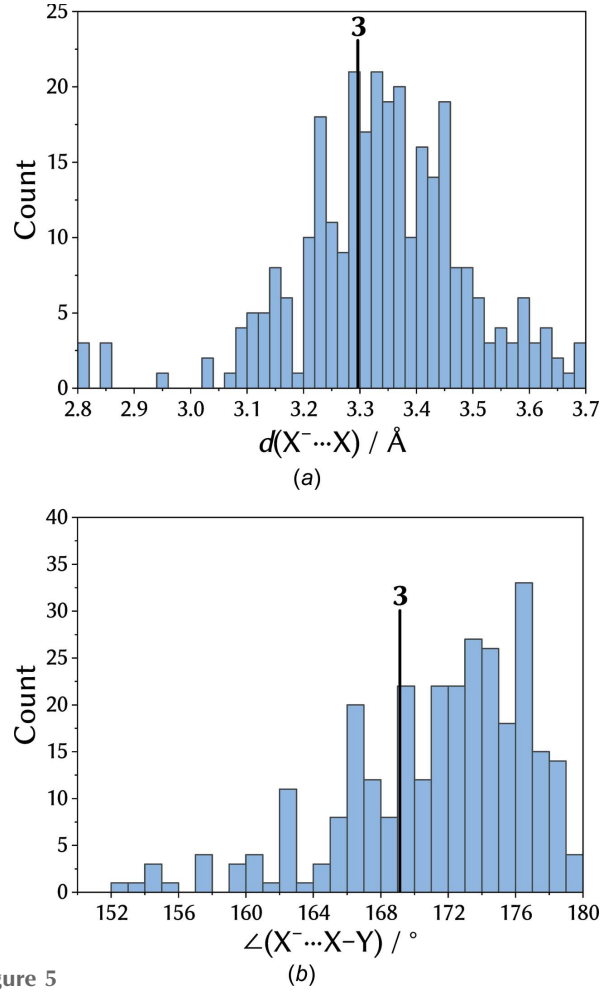

Figure 5
Histograms of the $X^-\cdots X$ distance and the $X^-\cdots X-Y$ angle of the first query run in the CSD, with **3** marked in black.

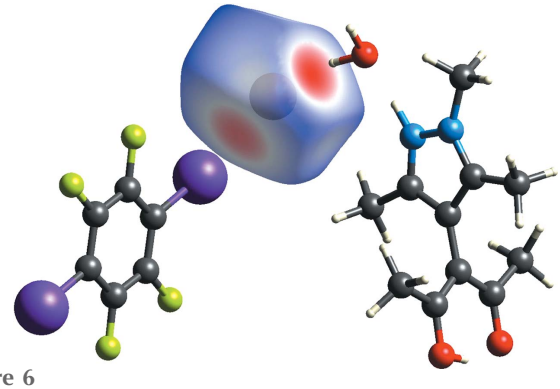

Figure 6
Hirshfeld surface (Spackman *et al.*, 2021) about Br1 mapped with d_{norm}; regions in red denote close contacts, while blue denotes long distances.

Table 3
Topological properties of important interactions of **3** at their bond critical point (3,−1).

BPL is bond path length, ρ is the electron density, G is the kinetic energy density, V the potential energy density and E is the total energy density in the bond critical point.

Bond	BPL (Å)	ρ (e Å^{-3})	$\nabla\rho$ (e Å^{-5})	G (a.u.)	G/ρ (a.u.)	V (a.u.)	E (a.u.)
I1···Br1	3.2981	0.119	1.11	0.0107	0.61	−0.00988	0.00083
Br1···H1O	2.4027	0.158	1.57	0.01684	0.72	−0.01739	−0.00054
Br1···O3^{i}	3.3112	0.182	1.18	0.01463	0.54	−0.01699	−0.00235
H2O···Br1^{ii}	2.4257	0.176	1.46	0.01692	0.65	−0.01874	−0.00181
O3···H1N	1.7698	0.424	2.1	0.04542	0.72	−0.06900	−0.02358
O···H—N^{a}	1.779 (4)	0.24 (2)	3.69 (3)	0.038	1.07	−0.038	

Note: (*a*) from CSD refcode ODEZOO01 for comparison (Şerb *et al.*, 2011). Symmetry codes: (i) $-x+2, y-\frac{1}{2}, -z+\frac{1}{2}$; (ii) $-x+2, y+\frac{1}{2}, -z+\frac{1}{2}$.

In order to gain insight into the electronic situation of **3**, the results of the diffraction experiment were used to calculate the electron density in a single-point calculation; details are provided in the supporting information. The topology of the calculated electron density was analyzed by Bader's Quantum Theory of Atoms in Molecules (QTAIM) (Bader, 1990). Covalent bonds and short contacts show up in the gradient of the electron density; two such trajectory plots are shown in Fig. 7 and show that, in addition to all covalent bonds, both classical N—H···O and O—H···Br hydrogen bonds exhibit almost linear bond paths and (3,−1) bond critical points (bcps) closer to the H atoms. A linear bond path and a bcp are also encountered for the C—I···Br halogen bond.

A synopsis of the relevant data for the electron density in the bcps of the secondary interactions is given in Table 3. For comparison, a previously published QTAIM analysis of the experimental electron density for an N—H···O hydrogen bond (CSD refcode ODEZOO01; Şerb *et al.*, 2011) has been appended to this table. Despite the similar hydrogen-bond geometry, the N—H···O contact in ODEZOO01 does not represent the dominant interaction; it is associated with significantly lower ρ_{bcp}, and the (positive) kinetic energy density G and the (negative) potential energy density V compensate to a negligible total energy density E, quite characteristic for weak closed-shell contacts (Espinosa *et al.*, 2002). The situation is distinctly different in **3**, where the interplay of G and V leads to a negative total energy density of −0.02358 a.u., by far the most relevant short contact in **3**. We are not aware of any experimental charge–density studies for O—H···Br or Br···I interactions which might be compared to the theoretical results for **3**. Fig. 8(*a*) shows the Laplacian of the electron density for **3** in the N/O/Br plane. A close look at the N—H···O hydrogen bond reveals the oxygen lone pair in the direction of the hydrogen-bond path, but no polarization of the Br^{-} ion towards the water H atom can be perceived. In Fig. 8(*b*), polarization of the bromide towards the σ-hole of I and the negatively polarized regions on I perpendicular to this Br···I contact show up.

In Fig. 9, the electrostatic potential (ESP) has been mapped on an isosurface of electron density; the orientations are the same as in the preceding Fig. 7. The H atoms attached to O or N atoms are associated with a distinctly positive potential

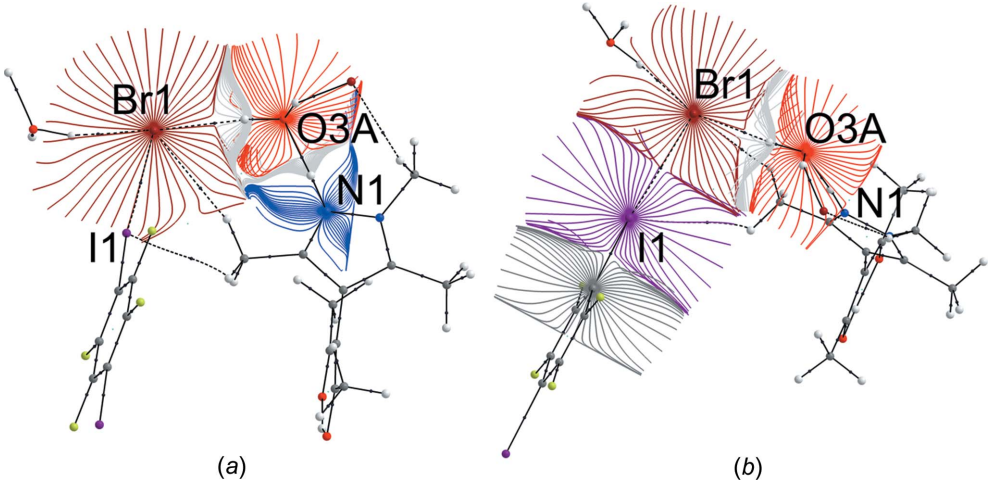

Figure 7
Trajectory plots (Keith, 2017) of **3**: (*a*) in the N/O/Br plane to reveal hydrogen bonds and (*b*) in the O/Br/I plane for the halogen bond. Intramolecular and conventional hydrogen-bond bond paths are shown as full black lines, while the halogen and nonclassical hydrogen bonds are shown as dashed black lines.

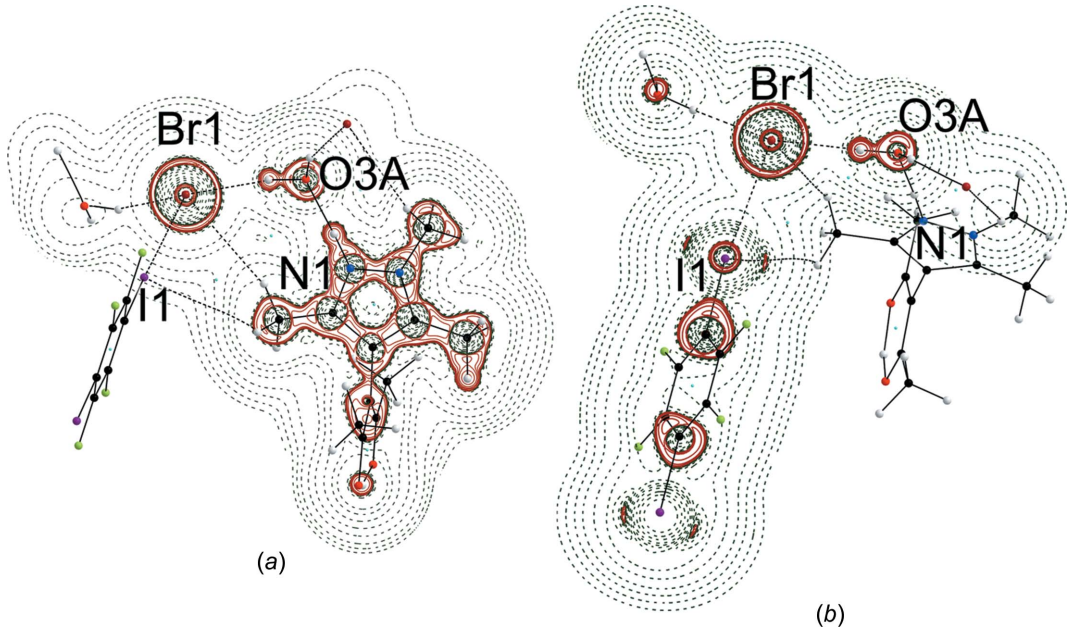

Figure 8
Laplacian of the electron density ρ in **3**; positive values are associated with dark-green dashed lines, while negative values are marked in red. Contour lines are drawn at $\pm 2^n \times 10^{-3}$ a.u. ($0 \leq n \leq 20$).

[Fig. 9(*a*)], and in Fig. 9(*b*), the positive σ-hole of the TFDIB I atom can be perceived.

4. Conclusion and outlook

In this contribution, we have evaluated the hydrochloride and hydrobromide of HacacMePz. The successful cocrystallization of the latter with TFDIB supports our earlier claim (van Terwingen *et al.*, 2021*a*) that the combination of hydrohalides with halogen-bond donors is not restricted to a lucky coincidence but is of broader relevance. As expected, the hydrogen and halogen bonds form an angle of roughly 90° around the bromide anion. We want to emphasize the predictability of the spatial arrangement of the two essential and highly directional short contacts. Considering the wide range of available Lewis bases and halogen-bond donors to which this rather underemployed concept may be applied, this combination may offer a new perspective for crystal engineering. We here only mention preliminary results from a closely related experiment; exchanging hydrobromic acid with hydrochloric acid leads to a different cocrystal of the composition HacacMePz·HCl·2TFDIB. In this compound, no water and a higher amount of TFDIB is present; the chloride anion accepts one hydrogen bond and three halogen bonds. In contrast to **3**, a 1D halogen-bonded chain is formed, which is not connected by hydrogen bonds in the second dimension. We are currently attempting to design cocrystals of hydrohalides of Lewis bases with XB donors in a rational way and will cover these results in a future contribution.

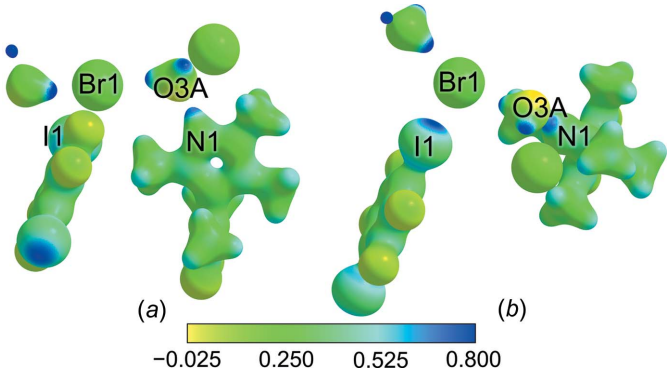

Figure 9
Electrostatical potential for **3** mapped onto the isosurface at an electron-density value of 0.05 a.u. (Keith, 2017); blue areas mark a positive potential (0.8 a.u.), yellow areas mark a negative potential (−0.025 a.u.) and green areas are associated with a potential of 0.25 a.u.

Acknowledgements

SvT gratefully acknowledges a fellowship for PhD students of RWTH Aachen University. The authors thank Simon Ernst for contributing to the experimental work for this submission. Open access funding enabled and organized by Projekt DEAL.

Funding information

Funding for this research was provided by: RWTH Graduiertenförderung (scholarship to SvT); Deutsche Forschungsgemeinschaft (grant No. EN 309/11-1 to RW).

References

Aakeröy, C. B., Champness, N. R. & Janiak, C. (2010). *CrystEngComm*, **12**, 22–43.
Aakeröy, C. B., Panikkattu, S., Chopade, P. D. & Desper, J. (2013). *CrystEngComm*, **15**, 3125–3136.

Abate, A., Biella, S., Cavallo, G., Meyer, F., Neukirch, H., Metrangolo, P., Pilati, T., Resnati, G. & Terraneo, G. (2009). *J. Fluor. Chem.* **130**, 1171–1177.
Abramov, Yu. A. (1997). *Acta Cryst.* A**53**, 264–272.
Allen, F. H. & Bruno, I. J. (2010). *Acta Cryst.* B**66**, 380–386.
Bader, R. F. W. (1990). In *Atoms in Molecules – A Quantum Theory*. Oxford: Clarendon Press.
Bianchi, R., Forni, A. & Pilati, T. (2003). *Chem. Eur. J.* **9**, 1631–1638.
Bianchi, R., Forni, A. & Pilati, T. (2004). *Acta Cryst.* B**60**, 559–568.
Blagden, N., de Matas, M., Gavan, P. T. & York, P. (2007). *Adv. Drug Deliv. Rev.* **59**, 617–630.
Bruker (2008). *SADABS*. Bruker AXS Inc., Madison, Wisconsin, USA.
Bruker (2009). *SMART* and *SAINT-Plus*. Bruker AXS Inc., Madison, Wisconsin, USA.
Cavallo, G., Metrangolo, P., Milani, R., Pilati, T., Priimagi, A., Resnati, G. & Terraneo, G. (2016). *Chem. Rev.* **116**, 2478–2601.
Clark, T., Hennemann, M., Murray, J. S. & Politzer, P. (2007). *J. Mol. Model.* **13**, 291–296.
Costa, P. J. (2018). *The Halogen bond: Nature and Applications* in *Chemical Synergies*, pp. 81–106. Berlin: De Gruyter.
Desiraju, G. R. (2010). *J. Chem. Sci.* **122**, 667–675.
Easton, R. E., Giesen, D. J., Welch, A., Cramer, C. J. & Truhlar, D. G. (1996). *Theor. Chim. Acta*, **93**, 281–301.
Espinosa, E., Alkorta, I., Elguero, J. & Molins, E. (2002). *J. Chem. Phys.* **117**, 5529–5542.
Espinosa, E., Lecomte, C. & Molins, E. (1999). *Chem. Phys. Lett.* **300**, 745–748.
Espinosa, E., Molins, E. & Lecomte, C. (1998). *Chem. Phys. Lett.* **285**, 170–173.
Etter, M. (1991). *J. Phys. Chem.* **95**, 4601–4610.
Frisch, M. J., *et al.* (2016). *GAUSSIAN16*. Revision C.01. Gaussian Inc., Wallingford, CT, USA. https://gaussian.com/.
Gao, M.-Y., Song, B.-Q., Sensharma, D. & Zaworotko, M. J. (2020). *SmartMat*, **2**, 38–55.
Groom, C. R., Bruno, I. J., Lightfoot, M. P. & Ward, S. C. (2016). *Acta Cryst.* B**72**, 171–179.
Keith, T. A. (2017). *AIMAll*. Version 17.01.25. TK Gristmill Software, Overland Park, KS, USA.
Kremer, M. & Englert, U. (2018). *Z. Kristallogr. Cryst. Mat.* **233**, 437–452.
Li, H., Eddaoudi, M., O'Keeffe, M. & Yaghi, O. M. (1999). *Nature*, **402**, 276–279.
Lu, T. & Chen, F. (2012). *J. Comput. Chem.* **33**, 580–592.
Lustig, W. P., Mukherjee, S., Rudd, N. D., Desai, A. V., Li, J. & Ghosh, S. K. (2017). *Chem. Soc. Rev.* **46**, 3242–3285.
Merkens, C., Pan, F. & Englert, U. (2013). *CrystEngComm*, **15**, 8153–8158.
Müller, P., Bon, V., Senkovska, I., Getzschmann, J., Weiss, M. S. & Kaskel, S. (2017). *Cryst. Growth Des.* **17**, 3221–3228.
O'Keeffe, M., Peskov, M. A., Ramsden, S. J. & Yaghi, O. M. (2008). *Acc. Chem. Res.* **41**, 1782–1789.
Otte, F., Kleinheider, J., Hiller, W., Wang, R., Englert, U. & Strohmann, C. (2021). *J. Am. Chem. Soc.* **143**, 4133–4137.
Politzer, P., Lane, P., Concha, M. C., Ma, Y. & Murray, J. S. (2007). *J. Mol. Model.* **13**, 305–311.
Politzer, P., Murray, J. S., Clark, T. & Resnati, G. (2017). *Phys. Chem. Chem. Phys.* **19**, 32166–32178.
Rimer, J. D., Chawla, A. & Le, T. T. (2018). *Annu. Rev. Chem. Biomol. Eng.* **9**, 283–309.
Robertson, C. C., Wright, J. S., Carrington, E. J., Perutz, R. N., Hunter, C. A. & Brammer, L. (2017). *Chem. Sci.* **8**, 5392–5398.
Saha, B. K., Nangia, A. & Jaskólski, M. (2005). *CrystEngComm*, **7**, 355–358.
Şerb, M.-D., Wang, R., Meven, M. & Englert, U. (2011). *Acta Cryst.* B**67**, 552–559.
Sheldrick, G. M. (2015*a*). *Acta Cryst.* A**71**, 3–8.
Sheldrick, G. M. (2015*b*). *Acta Cryst.* C**71**, 3–8.
Spackman, M. A. & Jayatilaka, D. (2009). *CrystEngComm*, **11**, 19–32.
Spackman, P. R., Turner, M. J., McKinnon, J. J., Wolff, S. K., Grimwood, D. J., Jayatilaka, D. & Spackman, M. A. (2021). *J. Appl. Cryst.* **54**, 1006–1011.
Spek, A. L. (2020). *Acta Cryst.* E**76**, 1–11.
van Terwingen, S., Brüx, D., Wang, R. & Englert, U. (2021*a*). *Molecules*, **26**, 3982.
van Terwingen, S., Nachtigall, N., Ebel, B. & Englert, U. (2021*b*). *Cryst. Growth Des.* **21**, 2962–2969.
Wang, R., Dols, T. S., Lehmann, C. W. & Englert, U. (2012). *Chem. Commun.* **48**, 6830–6832.
Wang, R., George, J., Potts, S. K., Kremer, M., Dronskowski, R. & Englert, U. (2019). *Acta Cryst.* C**75**, 1190–1201.
Wang, R., Hartnick, D. & Englert, U. (2018*a*). *Z. Kristallogr.* **233**, 733–744.
Wang, R., Kalf, I. & Englert, U. (2018*b*). *RSC Adv.* **8**, 34287–34290.
Wu, H. Q., Yan, C. S., Luo, F. & Krishna, R. (2018). *Inorg. Chem.* **57**, 3679–3682.
Zhang, C., Jiao, F. & Li, H. (2018). *Cryst. Growth Des.* **18**, 5713–5726.

supporting information

Acta Cryst. (2022). C**78**, 324-331 [https://doi.org/10.1107/S2053229622004648]

Weaving a 2D net of hydrogen and halogen bonds: cocrystal of a pyrazolium bromide with tetrafluorodiiodobenzene

Steven van Terwingen, Ben Ebel, Ruimin Wang and Ulli Englert

Computing details

For all structures, data collection: *SMART* (Bruker, 2009); cell refinement: *SAINT* (Bruker, 2009); data reduction: *SAINT* (Bruker, 2009); program(s) used to solve structure: SHELXT2014 (Sheldrick, 2015*a*); program(s) used to refine structure: *SHELXL2018* (Sheldrick, 2015*b*); molecular graphics: *PLATON* (Spek, 2020).

4-(2-Hydroxy-4-oxopent-2-en-3-yl)-1,3,5-trimethyl-1*H*-pyrazol-2-ium chloride (1)

Crystal data

$C_{11}H_{17}N_2O_2^+\cdot Cl^-$
M_r = 244.71
Orthorhombic, *Pbca*
a = 8.770 (2) Å
b = 11.658 (3) Å
c = 23.843 (6) Å
V = 2437.9 (11) Å^3
Z = 8
$F(000)$ = 1040
D_x = 1.333 Mg m^{-3}
Mo $K\alpha$ radiation, λ = 0.71073 Å
Cell parameters from 3014 reflections
θ = 2.9–24.4°
μ = 0.30 mm^{-1}
T = 100 K
Block, colorless
0.34 × 0.17 × 0.14 mm

Data collection

Bruker APEX CCD diffractometer
Radiation source: microsource
Multilayer optics monochromator
ω scans
Absorption correction: multi-scan (SADABS; Bruker, 2008)
T_{min} = 0.619, T_{max} = 0.746
32185 measured reflections
3104 independent reflections
2482 reflections with $I > 2\sigma(I)$
R_{int} = 0.088
θ_{max} = 28.7°, θ_{min} = 1.7°
h = −11→11
k = −15→15
l = −31→32

Refinement

Refinement on F^2
Least-squares matrix: full
$R[F^2 > 2\sigma(F^2)]$ = 0.042
$wR(F^2)$ = 0.112
S = 1.05
3104 reflections
156 parameters
0 restraints
Primary atom site location: dual
Hydrogen site location: mixed
H atoms treated by a mixture of independent and constrained refinement
$w = 1/[\sigma^2(F_o^2) + (0.0452P)^2 + 1.6349P]$ where $P = (F_o^2 + 2F_c^2)/3$
$(\Delta/\sigma)_{max}$ = 0.001
$\Delta\rho_{max}$ = 0.39 e Å^{-3}
$\Delta\rho_{min}$ = −0.34 e Å^{-3}

Special details

Geometry. All e.s.d.'s (except the e.s.d. in the dihedral angle between two l.s. planes) are estimated using the full covariance matrix. The cell e.s.d.'s are taken into account individually in the estimation of e.s.d.'s in distances, angles and torsion angles; correlations between e.s.d.'s in cell parameters are only used when they are defined by crystal symmetry. An approximate (isotropic) treatment of cell e.s.d.'s is used for estimating e.s.d.'s involving l.s. planes.

Refinement. Data was integrated with *SAINT* (Bruker, 2009) and corrected for absorption by multi-scan methods with *SADABS* (Bruker, 2008). The structures were solved by intrinsic phasing (Sheldrick, 2015) and refined by full-matrix least-squares procedures against F^2, as implemented in *SHELXL18* (Sheldrick, 2015). CIFs have been deposited under CCDC identifiers *X*.

Fractional atomic coordinates and isotropic or equivalent isotropic displacement parameters (Å²)

	x	*y*	*z*	U_{iso}*/U_{eq}
Cl1	0.48366 (5)	0.21934 (4)	0.55313 (2)	0.02320 (13)
O1	0.67930 (14)	0.41256 (11)	0.22096 (5)	0.0200 (3)
H1	0.610 (3)	0.470 (2)	0.2146 (9)	0.030*
O2	0.48808 (14)	0.56270 (11)	0.23607 (5)	0.0206 (3)
N1	0.55770 (16)	0.37180 (12)	0.45728 (6)	0.0158 (3)
H1N	0.531 (2)	0.3259 (19)	0.4865 (9)	0.024*
N2	0.67005 (15)	0.45031 (12)	0.46203 (6)	0.0160 (3)
C1	0.7955 (2)	0.30729 (16)	0.29401 (7)	0.0216 (4)
H1A	0.743497	0.232910	0.294617	0.032*
H1B	0.832500	0.325599	0.331755	0.032*
H1C	0.882014	0.303829	0.268037	0.032*
C2	0.68699 (18)	0.39780 (14)	0.27521 (7)	0.0167 (3)
C3	0.59660 (18)	0.46151 (14)	0.31165 (7)	0.0151 (3)
C4	0.49527 (18)	0.54526 (14)	0.28871 (7)	0.0165 (3)
C5	0.3949 (2)	0.61467 (15)	0.32626 (7)	0.0207 (4)
H5A	0.337861	0.670508	0.303818	0.031*
H5B	0.457633	0.655214	0.353899	0.031*
H5C	0.323324	0.563815	0.345710	0.031*
C6	0.39044 (19)	0.28681 (15)	0.38492 (7)	0.0204 (4)
H6A	0.351511	0.243709	0.417170	0.031*
H6B	0.430135	0.233213	0.356818	0.031*
H6C	0.307726	0.332195	0.368449	0.031*
C7	0.51479 (17)	0.36466 (14)	0.40360 (7)	0.0153 (3)
C8	0.60356 (17)	0.44124 (14)	0.37277 (7)	0.0149 (3)
C9	0.70177 (18)	0.49287 (14)	0.41126 (7)	0.0158 (3)
C10	0.8252 (2)	0.57779 (16)	0.40236 (8)	0.0232 (4)
H10A	0.793639	0.652286	0.417459	0.035*
H10B	0.845695	0.585203	0.362119	0.035*
H10C	0.917767	0.552030	0.421609	0.035*
C11	0.7473 (2)	0.46977 (16)	0.51530 (7)	0.0203 (4)
H11A	0.841121	0.424176	0.516587	0.030*
H11B	0.680172	0.446905	0.546192	0.030*
H11C	0.772600	0.551310	0.518932	0.030*

Atomic displacement parameters (Å²)

	U^{11}	U^{22}	U^{33}	U^{12}	U^{13}	U^{23}
Cl1	0.0271 (2)	0.0250 (2)	0.0176 (2)	−0.00843 (17)	−0.00033 (16)	0.00184 (16)
O1	0.0198 (6)	0.0246 (6)	0.0157 (6)	0.0015 (5)	0.0013 (5)	0.0003 (5)
O2	0.0226 (6)	0.0237 (6)	0.0157 (6)	0.0011 (5)	−0.0023 (5)	0.0020 (5)
N1	0.0149 (6)	0.0166 (7)	0.0158 (7)	−0.0008 (5)	−0.0003 (5)	0.0014 (5)
N2	0.0144 (6)	0.0181 (7)	0.0154 (7)	0.0002 (5)	−0.0019 (5)	−0.0010 (5)
C1	0.0200 (8)	0.0223 (9)	0.0225 (8)	0.0043 (7)	0.0013 (7)	−0.0011 (7)
C2	0.0147 (8)	0.0182 (8)	0.0172 (8)	−0.0032 (6)	−0.0002 (6)	0.0006 (6)
C3	0.0135 (7)	0.0168 (8)	0.0151 (7)	−0.0019 (6)	−0.0007 (6)	0.0006 (6)
C4	0.0157 (8)	0.0160 (8)	0.0178 (8)	−0.0031 (6)	−0.0016 (6)	0.0003 (6)
C5	0.0221 (8)	0.0207 (8)	0.0193 (8)	0.0054 (7)	−0.0021 (7)	−0.0008 (7)
C6	0.0181 (8)	0.0205 (8)	0.0225 (8)	−0.0045 (6)	−0.0022 (7)	0.0027 (7)
C7	0.0134 (7)	0.0158 (7)	0.0166 (7)	0.0020 (6)	0.0000 (6)	0.0009 (6)
C8	0.0126 (7)	0.0159 (8)	0.0161 (8)	0.0019 (6)	−0.0009 (6)	−0.0004 (6)
C9	0.0150 (7)	0.0156 (7)	0.0167 (8)	0.0019 (6)	−0.0008 (6)	−0.0002 (6)
C10	0.0223 (9)	0.0234 (9)	0.0238 (9)	−0.0076 (7)	−0.0036 (7)	0.0018 (7)
C11	0.0205 (8)	0.0250 (9)	0.0155 (7)	0.0030 (7)	−0.0046 (6)	−0.0035 (7)

Geometric parameters (Å, º)

O1—C2	1.307 (2)	C5—H5A	0.9800
O1—H1	0.91 (2)	C5—H5B	0.9800
O2—C4	1.273 (2)	C5—H5C	0.9800
N1—C7	1.337 (2)	C6—C7	1.487 (2)
N1—N2	1.3496 (19)	C6—H6A	0.9800
N1—H1N	0.91 (2)	C6—H6B	0.9800
N2—C9	1.338 (2)	C6—H6C	0.9800
N2—C11	1.457 (2)	C7—C8	1.394 (2)
C1—C2	1.490 (2)	C8—C9	1.395 (2)
C1—H1A	0.9800	C9—C10	1.482 (2)
C1—H1B	0.9800	C10—H10A	0.9800
C1—H1C	0.9800	C10—H10B	0.9800
C2—C3	1.391 (2)	C10—H10C	0.9800
C3—C4	1.429 (2)	C11—H11A	0.9800
C3—C8	1.478 (2)	C11—H11B	0.9800
C4—C5	1.494 (2)	C11—H11C	0.9800
C2—O1—H1	107.1 (14)	C7—C6—H6A	109.5
C7—N1—N2	109.17 (13)	C7—C6—H6B	109.5
C7—N1—H1N	128.7 (14)	H6A—C6—H6B	109.5
N2—N1—H1N	121.5 (13)	C7—C6—H6C	109.5
C9—N2—N1	109.11 (13)	H6A—C6—H6C	109.5
C9—N2—C11	129.37 (15)	H6B—C6—H6C	109.5
N1—N2—C11	121.22 (14)	N1—C7—C8	107.92 (14)
C2—C1—H1A	109.5	N1—C7—C6	122.10 (15)
C2—C1—H1B	109.5	C8—C7—C6	129.98 (15)

H1A—C1—H1B	109.5	C7—C8—C9	105.92 (14)
C2—C1—H1C	109.5	C7—C8—C3	126.82 (15)
H1A—C1—H1C	109.5	C9—C8—C3	127.25 (15)
H1B—C1—H1C	109.5	N2—C9—C8	107.87 (14)
O1—C2—C3	121.24 (15)	N2—C9—C10	121.96 (15)
O1—C2—C1	115.10 (15)	C8—C9—C10	130.15 (15)
C3—C2—C1	123.65 (15)	C9—C10—H10A	109.5
C2—C3—C4	118.69 (15)	C9—C10—H10B	109.5
C2—C3—C8	120.48 (15)	H10A—C10—H10B	109.5
C4—C3—C8	120.82 (14)	C9—C10—H10C	109.5
O2—C4—C3	121.15 (15)	H10A—C10—H10C	109.5
O2—C4—C5	118.37 (15)	H10B—C10—H10C	109.5
C3—C4—C5	120.48 (15)	N2—C11—H11A	109.5
C4—C5—H5A	109.5	N2—C11—H11B	109.5
C4—C5—H5B	109.5	H11A—C11—H11B	109.5
H5A—C5—H5B	109.5	N2—C11—H11C	109.5
C4—C5—H5C	109.5	H11A—C11—H11C	109.5
H5A—C5—H5C	109.5	H11B—C11—H11C	109.5
H5B—C5—H5C	109.5		

Hydrogen-bond geometry (Å, º)

D—H···*A*	*D*—H	H···*A*	*D*···*A*	*D*—H···*A*
O1—H1···O2	0.91 (2)	1.61 (2)	2.4507 (18)	152 (2)
N1—H1*N*···Cl1	0.91 (2)	2.06 (2)	2.9671 (16)	176.7 (19)

4-(2-Hydroxy-4-oxopent-2-en-3-yl)-1,3,5-trimethyl-1*H*-pyrazol-2-ium bromide (2)

Crystal data

$C_{11}H_{17}N_2O_2^+ \cdot Br^-$
M_r = 289.17
Orthorhombic, *Pbca*
a = 8.859 (4) Å
b = 12.038 (5) Å
c = 23.805 (10) Å
V = 2538.7 (18) Å^3
Z = 8
$F(000)$ = 1184
D_x = 1.513 Mg m^{-3}
Mo $K\alpha$ radiation, λ = 0.71073 Å
Cell parameters from 1801 reflections
θ = 2.9–23.7°
μ = 3.23 mm^{-1}
T = 100 K
Block, colorless
0.13 × 0.06 × 0.03 mm

Data collection

Bruker APEX CCD diffractometer
Radiation source: microsource
Multilayer optics monochromator
ω scans
Absorption correction: multi-scan (SADABS; Bruker, 2008)
T_{min} = 0.595, T_{max} = 0.745
26167 measured reflections
2321 independent reflections
1647 reflections with $I > 2\sigma(I)$
R_{int} = 0.096
θ_{max} = 25.4°, θ_{min} = 2.9°
h = −10→10
k = −14→14
l = −28→28

Refinement

Refinement on F^2
Least-squares matrix: full
$R[F^2 > 2\sigma(F^2)] = 0.037$
$wR(F^2) = 0.099$
$S = 1.03$
2321 reflections
156 parameters
1 restraint
Primary atom site location: dual
Hydrogen site location: mixed
H atoms treated by a mixture of independent and constrained refinement
$w = 1/[\sigma^2(F_o^2) + (0.0363P)^2 + 4.2695P]$ where $P = (F_o^2 + 2F_c^2)/3$
$(\Delta/\sigma)_{max} = 0.001$
$\Delta\rho_{max} = 0.57$ e Å^{-3}
$\Delta\rho_{min} = -0.58$ e Å^{-3}

Special details

Geometry. All e.s.d.'s (except the e.s.d. in the dihedral angle between two l.s. planes) are estimated using the full covariance matrix. The cell e.s.d.'s are taken into account individually in the estimation of e.s.d.'s in distances, angles and torsion angles; correlations between e.s.d.'s in cell parameters are only used when they are defined by crystal symmetry. An approximate (isotropic) treatment of cell e.s.d.'s is used for estimating e.s.d.'s involving l.s. planes.

Refinement. Data was integrated with *SAINT* (Bruker, 2009) and corrected for absorption by multi-scan methods with *SADABS* (Bruker, 2008). The structures were solved by intrinsic phasing (Sheldrick, 2015) and refined by full-matrix least-squares procedures against F^2, as implemented in *SHELXL18* (Sheldrick, 2015). CIFs have been deposited under CCDC identifiers *X*.

Fractional atomic coordinates and isotropic or equivalent isotropic displacement parameters (Å²)

	x	*y*	*z*	U_{iso}*/U_{eq}
Br1	0.49971 (4)	0.20029 (3)	0.55685 (2)	0.02110 (15)
O1	0.6800 (3)	0.4078 (2)	0.21800 (10)	0.0216 (6)
H1	0.611 (4)	0.460 (3)	0.2129 (17)	0.032*
O2	0.4896 (3)	0.5558 (2)	0.23314 (10)	0.0224 (6)
N1	0.5571 (3)	0.3617 (3)	0.45444 (13)	0.0161 (6)
H1N	0.534 (5)	0.313 (3)	0.4838 (18)	0.024*
N2	0.6585 (3)	0.4451 (2)	0.46080 (12)	0.0160 (6)
C1	0.7928 (4)	0.3056 (3)	0.29197 (16)	0.0214 (9)
H1A	0.741378	0.233562	0.292093	0.032*
H1B	0.827930	0.322966	0.330012	0.032*
H1C	0.879453	0.302609	0.266406	0.032*
C2	0.6859 (4)	0.3935 (3)	0.27278 (14)	0.0175 (8)
C3	0.5953 (4)	0.4555 (3)	0.30897 (14)	0.0144 (7)
C4	0.4958 (4)	0.5384 (3)	0.28592 (15)	0.0177 (7)
C5	0.3974 (4)	0.6068 (3)	0.32370 (15)	0.0210 (8)
H5A	0.335758	0.657283	0.300967	0.031*
H5B	0.460722	0.650082	0.349375	0.031*
H5C	0.331301	0.557663	0.345451	0.031*
C6	0.4057 (4)	0.2711 (3)	0.37965 (15)	0.0206 (8)
H6A	0.382842	0.218494	0.409882	0.031*
H6B	0.447140	0.230860	0.347371	0.031*
H6C	0.313051	0.309635	0.368402	0.031*
C7	0.5191 (4)	0.3544 (3)	0.40001 (15)	0.0159 (8)
C8	0.5998 (4)	0.4351 (3)	0.37032 (14)	0.0148 (7)
C9	0.6881 (4)	0.4899 (3)	0.41042 (15)	0.0171 (8)
C10	0.8022 (4)	0.5799 (3)	0.40332 (15)	0.0211 (8)

H10A	0.758786	0.650787	0.415482	0.032*
H10B	0.831351	0.584958	0.363695	0.032*
H10C	0.891390	0.562995	0.426119	0.032*
C11	0.7281 (4)	0.4669 (3)	0.51589 (15)	0.0203 (8)
H11A	0.822524	0.424956	0.518996	0.030*
H11B	0.658764	0.443650	0.545752	0.030*
H11C	0.749179	0.546439	0.519574	0.030*

Atomic displacement parameters (Å²)

	U^{11}	U^{22}	U^{33}	U^{12}	U^{13}	U^{23}
Br1	0.0193 (2)	0.0250 (2)	0.0190 (2)	−0.00499 (17)	0.00065 (16)	0.00112 (14)
O1	0.0160 (14)	0.0310 (16)	0.0177 (13)	0.0033 (11)	0.0015 (11)	0.0013 (11)
O2	0.0203 (14)	0.0294 (14)	0.0176 (13)	0.0039 (12)	−0.0024 (11)	0.0036 (11)
N1	0.0106 (14)	0.0210 (17)	0.0168 (16)	0.0002 (13)	0.0022 (12)	0.0017 (14)
N2	0.0148 (15)	0.0185 (15)	0.0146 (15)	0.0004 (13)	−0.0005 (12)	−0.0005 (13)
C1	0.018 (2)	0.025 (2)	0.021 (2)	0.0026 (17)	0.0021 (16)	−0.0004 (16)
C2	0.0110 (17)	0.0235 (19)	0.0179 (19)	−0.0056 (15)	−0.0021 (14)	0.0014 (15)
C3	0.0100 (17)	0.0175 (18)	0.0156 (18)	−0.0022 (14)	−0.0018 (14)	−0.0003 (15)
C4	0.0128 (17)	0.0183 (17)	0.0219 (18)	−0.0050 (16)	−0.0025 (15)	0.0020 (14)
C5	0.0194 (19)	0.022 (2)	0.0211 (19)	0.0065 (16)	−0.0018 (15)	−0.0015 (16)
C6	0.016 (2)	0.025 (2)	0.0208 (19)	−0.0035 (16)	−0.0020 (15)	0.0030 (16)
C7	0.0090 (18)	0.0204 (18)	0.0182 (18)	0.0030 (14)	0.0002 (14)	0.0001 (15)
C8	0.0067 (16)	0.0195 (19)	0.0183 (18)	0.0020 (14)	−0.0006 (14)	0.0006 (15)
C9	0.0102 (17)	0.0204 (19)	0.0208 (19)	0.0046 (15)	−0.0009 (14)	0.0013 (15)
C10	0.0184 (19)	0.023 (2)	0.022 (2)	−0.0030 (16)	−0.0037 (16)	0.0018 (16)
C11	0.0169 (19)	0.028 (2)	0.0158 (18)	0.0041 (16)	−0.0046 (15)	−0.0032 (15)

Geometric parameters (Å, º)

O1—C2	1.316 (4)	C5—H5A	0.9800
O1—H1	0.884 (19)	C5—H5B	0.9800
O2—C4	1.275 (4)	C5—H5C	0.9800
N1—C7	1.342 (5)	C6—C7	1.499 (5)
N1—N2	1.356 (4)	C6—H6A	0.9800
N1—H1N	0.93 (4)	C6—H6B	0.9800
N2—C9	1.341 (4)	C6—H6C	0.9800
N2—C11	1.472 (4)	C7—C8	1.398 (5)
C1—C2	1.492 (5)	C8—C9	1.400 (5)
C1—H1A	0.9800	C9—C10	1.490 (5)
C1—H1B	0.9800	C10—H10A	0.9800
C1—H1C	0.9800	C10—H10B	0.9800
C2—C3	1.394 (5)	C10—H10C	0.9800
C3—C4	1.440 (5)	C11—H11A	0.9800
C3—C8	1.482 (5)	C11—H11B	0.9800
C4—C5	1.499 (5)	C11—H11C	0.9800
C2—O1—H1	105 (3)	C7—C6—H6A	109.5

C7—N1—N2	108.8 (3)	C7—C6—H6B	109.5
C7—N1—H1N	129 (3)	H6A—C6—H6B	109.5
N2—N1—H1N	122 (3)	C7—C6—H6C	109.5
C9—N2—N1	109.1 (3)	H6A—C6—H6C	109.5
C9—N2—C11	130.0 (3)	H6B—C6—H6C	109.5
N1—N2—C11	120.6 (3)	N1—C7—C8	108.3 (3)
C2—C1—H1A	109.5	N1—C7—C6	121.6 (3)
C2—C1—H1B	109.5	C8—C7—C6	130.1 (3)
H1A—C1—H1B	109.5	C7—C8—C9	105.6 (3)
C2—C1—H1C	109.5	C7—C8—C3	126.9 (3)
H1A—C1—H1C	109.5	C9—C8—C3	127.5 (3)
H1B—C1—H1C	109.5	N2—C9—C8	108.1 (3)
O1—C2—C3	121.3 (3)	N2—C9—C10	121.8 (3)
O1—C2—C1	114.9 (3)	C8—C9—C10	130.1 (3)
C3—C2—C1	123.8 (3)	C9—C10—H10A	109.5
C2—C3—C4	119.2 (3)	C9—C10—H10B	109.5
C2—C3—C8	120.3 (3)	H10A—C10—H10B	109.5
C4—C3—C8	120.5 (3)	C9—C10—H10C	109.5
O2—C4—C3	121.0 (3)	H10A—C10—H10C	109.5
O2—C4—C5	118.5 (3)	H10B—C10—H10C	109.5
C3—C4—C5	120.5 (3)	N2—C11—H11A	109.5
C4—C5—H5A	109.5	N2—C11—H11B	109.5
C4—C5—H5B	109.5	H11A—C11—H11B	109.5
H5A—C5—H5B	109.5	N2—C11—H11C	109.5
C4—C5—H5C	109.5	H11A—C11—H11C	109.5
H5A—C5—H5C	109.5	H11B—C11—H11C	109.5
H5B—C5—H5C	109.5		

Hydrogen-bond geometry (Å, º)

D—H···*A*	*D*—H	H···*A*	*D*···*A*	*D*—H···*A*
O1—H1···O2	0.88 (2)	1.65 (2)	2.479 (4)	155 (4)
N1—H1*N*···Br1	0.93 (4)	2.23 (4)	3.159 (3)	174 (4)

4-(2-Hydroxy-4-oxopent-2-en-3-yl)-1,3,5-trimethyl-1*H*-pyrazol-2-ium bromide–1,2,4,5-tetrafluoro-3,6-diiodobenzene–water (2/1/2) (3)

Crystal data

$C_{11}H_{17}N_2O_2^+\cdot Br^-\cdot 0.5C_6F_4I_2\cdot H_2O$
M_r = 508.12
Monoclinic, $P2_1/c$
a = 12.9151 (2) Å
b = 11.3061 (2) Å
c = 12.5239 (2) Å
β = 90.6281 (5)°
V = 1828.62 (5) Å^3
Z = 4
$F(000)$ = 988
D_x = 1.846 Mg m^{-3}
Mo $K\alpha$ radiation, λ = 0.71073 Å
Cell parameters from 9900 reflections
θ = 2.4–44.8°
μ = 3.97 mm^{-1}
T = 100 K
Block, colorless
0.19 × 0.15 × 0.08 mm

Data collection

Bruker APEX CCD diffractometer
Radiation source: microsource
Multilayer optics monochromator
ω scans
Absorption correction: multi-scan (SADABS; Bruker, 2008)
T_{min} = 0.563, T_{max} = 0.749
170884 measured reflections
15145 independent reflections
11531 reflections with $I > 2\sigma(I)$
R_{int} = 0.091
θ_{max} = 45.2°, θ_{min} = 1.6°
h = −25→25
k = −21→22
l = −24→24

Refinement

Refinement on F^2
Least-squares matrix: full
$R[F^2 > 2\sigma(F^2)]$ = 0.042
$wR(F^2)$ = 0.093
S = 1.10
15145 reflections
235 parameters
5 restraints
Primary atom site location: dual
Hydrogen site location: mixed
H atoms treated by a mixture of independent and constrained refinement
$w = 1/[\sigma^2(F_o^2) + (0.0278P)^2 + 1.1016P]$ where $P = (F_o^2 + 2F_c^2)/3$
$(\Delta/\sigma)_{max}$ = 0.004
$\Delta\rho_{max}$ = 1.19 e Å^{-3}
$\Delta\rho_{min}$ = −0.78 e Å^{-3}

Special details

Geometry. All e.s.d.'s (except the e.s.d. in the dihedral angle between two l.s. planes) are estimated using the full covariance matrix. The cell e.s.d.'s are taken into account individually in the estimation of e.s.d.'s in distances, angles and torsion angles; correlations between e.s.d.'s in cell parameters are only used when they are defined by crystal symmetry. An approximate (isotropic) treatment of cell e.s.d.'s is used for estimating e.s.d.'s involving l.s. planes.

Refinement. Data was integrated with *SAINT* (Bruker, 2009) and corrected for absorption by multi-scan methods with *SADABS* (Bruker, 2008). The structures were solved by intrinsic phasing (Sheldrick, 2015) and refined by full-matrix least-squares procedures against F^2, as implemented in *SHELXL18* (Sheldrick, 2015). CIFs have been deposited under CCDC identifiers *X*.

Fractional atomic coordinates and isotropic or equivalent isotropic displacement parameters (Å^2)

	x	*y*	*z*	U_{iso}*/U_{eq}	Occ. (<1)
I1	0.73674 (2)	0.41461 (2)	0.11625 (2)	0.02081 (3)	
Br1	0.97406 (2)	0.38714 (2)	0.21245 (2)	0.02397 (4)	
F1	0.67254 (9)	0.63142 (11)	−0.03307 (10)	0.0282 (2)	
F2	0.50517 (9)	0.30380 (10)	0.12555 (9)	0.0268 (2)	
O1	0.46657 (11)	0.48290 (15)	0.69217 (13)	0.0307 (3)	
H1	0.498 (3)	0.429 (3)	0.735 (2)	0.046*	
O2	0.59044 (13)	0.36408 (13)	0.79672 (12)	0.0313 (3)	
N1	0.85864 (11)	0.61853 (13)	0.51320 (11)	0.0193 (2)	
N2	0.85211 (10)	0.70749 (12)	0.58490 (10)	0.0178 (2)	
C1	0.51657 (15)	0.63681 (19)	0.57551 (17)	0.0283 (3)	
H1A	0.454428	0.614524	0.534657	0.042*	
H1B	0.573895	0.650592	0.526420	0.042*	
H1C	0.502878	0.709230	0.615968	0.042*	
C2	0.54480 (13)	0.53933 (16)	0.65098 (14)	0.0233 (3)	
C3	0.64711 (13)	0.51070 (14)	0.67724 (12)	0.0195 (2)	
C4	0.66549 (16)	0.41981 (15)	0.75456 (14)	0.0238 (3)	
C5	0.77267 (18)	0.38794 (18)	0.79002 (16)	0.0299 (4)	

H5A	0.769346	0.337107	0.853273	0.045*	
H5B	0.811254	0.460117	0.807605	0.045*	
H5C	0.807743	0.345672	0.732459	0.045*	
C6	0.77563 (16)	0.42831 (18)	0.46744 (16)	0.0285 (4)	
H6A	0.723646	0.443544	0.411526	0.043*	
H6B	0.753163	0.361695	0.511570	0.043*	
H6C	0.842007	0.409125	0.434459	0.043*	
C7	0.78788 (12)	0.53556 (14)	0.53547 (12)	0.0186 (2)	
C8	0.73404 (12)	0.57282 (13)	0.62543 (12)	0.0175 (2)	
C9	0.77738 (12)	0.68216 (14)	0.65480 (12)	0.0183 (2)	
C10	0.75123 (16)	0.76026 (16)	0.74613 (15)	0.0267 (3)	
H10A	0.803194	0.750493	0.803064	0.040*	
H10B	0.682820	0.738923	0.773213	0.040*	
H10C	0.750445	0.842826	0.722332	0.040*	
O3A	1.00897 (12)	0.61454 (14)	0.37201 (13)	0.0262 (3)	0.911 (4)
H1OA	1.002 (3)	0.565 (3)	0.320 (2)	0.039*	0.911 (4)
H2OA	1.017 (3)	0.678 (2)	0.335 (2)	0.039*	0.911 (4)
C11A	0.92489 (15)	0.80766 (17)	0.57991 (16)	0.0232 (3)	0.911 (4)
H11A	0.902248	0.870205	0.628538	0.035*	0.911 (4)
H11B	0.926528	0.838496	0.506820	0.035*	0.911 (4)
H11C	0.994315	0.780886	0.601060	0.035*	0.911 (4)
H1NA	0.909 (2)	0.622 (3)	0.465 (2)	0.029*	0.911 (4)
O3B	0.9886 (11)	0.8766 (13)	0.5562 (12)	0.023 (3)*	0.089 (4)
H1OB	0.984879	0.937116	0.596307	0.034*	0.089 (4)
H2OB	0.997932	0.879197	0.489170	0.034*	0.089 (4)
C11B	0.9465 (17)	0.6060 (19)	0.4390 (17)	0.025 (4)*	0.089 (4)
H11D	0.995758	0.547881	0.467638	0.037*	0.089 (4)
H11E	0.981147	0.682510	0.431006	0.037*	0.089 (4)
H11F	0.920604	0.579215	0.369206	0.037*	0.089 (4)
H1NB	0.896235	0.762217	0.575569	0.029*	0.089 (4)
C12	0.58783 (13)	0.56515 (15)	−0.01557 (13)	0.0199 (2)	
C13	0.59468 (12)	0.46488 (14)	0.04826 (12)	0.0188 (2)	
C14	0.50476 (13)	0.40086 (14)	0.06350 (12)	0.0191 (2)	

Atomic displacement parameters (Å²)

	U^{11}	U^{22}	U^{33}	U^{12}	U^{13}	U^{23}
I1	0.02104 (4)	0.02089 (5)	0.02042 (4)	0.00294 (3)	−0.00322 (3)	−0.00171 (3)
Br1	0.02419 (7)	0.02176 (7)	0.02585 (8)	0.00514 (6)	−0.00477 (6)	−0.00142 (6)
F1	0.0227 (5)	0.0302 (6)	0.0315 (5)	−0.0069 (4)	−0.0026 (4)	0.0069 (4)
F2	0.0309 (5)	0.0222 (5)	0.0272 (5)	−0.0026 (4)	−0.0053 (4)	0.0084 (4)
O1	0.0243 (6)	0.0336 (7)	0.0345 (7)	−0.0083 (5)	0.0103 (5)	−0.0075 (6)
O2	0.0438 (8)	0.0241 (6)	0.0264 (6)	−0.0107 (6)	0.0125 (6)	−0.0007 (5)
N1	0.0177 (5)	0.0211 (6)	0.0192 (5)	−0.0008 (4)	0.0036 (4)	−0.0015 (4)
N2	0.0178 (5)	0.0179 (5)	0.0176 (5)	0.0000 (4)	0.0015 (4)	0.0008 (4)
C1	0.0220 (7)	0.0287 (9)	0.0341 (9)	0.0037 (6)	0.0011 (6)	−0.0030 (7)
C2	0.0218 (7)	0.0242 (7)	0.0242 (7)	−0.0029 (5)	0.0066 (5)	−0.0068 (5)
C3	0.0224 (6)	0.0175 (6)	0.0187 (6)	−0.0020 (5)	0.0048 (5)	−0.0008 (4)

C4	0.0332 (8)	0.0186 (6)	0.0198 (6)	−0.0023 (6)	0.0060 (6)	−0.0022 (5)
C5	0.0393 (10)	0.0249 (8)	0.0257 (8)	0.0020 (7)	0.0016 (7)	0.0046 (6)
C6	0.0286 (8)	0.0289 (9)	0.0283 (8)	−0.0064 (6)	0.0077 (6)	−0.0111 (6)
C7	0.0184 (6)	0.0201 (6)	0.0174 (5)	−0.0005 (5)	0.0013 (4)	−0.0015 (4)
C8	0.0185 (6)	0.0167 (6)	0.0172 (5)	−0.0001 (4)	0.0024 (4)	0.0004 (4)
C9	0.0206 (6)	0.0171 (6)	0.0173 (5)	0.0006 (4)	0.0021 (4)	0.0013 (4)
C10	0.0355 (9)	0.0205 (7)	0.0242 (7)	−0.0037 (6)	0.0087 (6)	−0.0036 (5)
O3A	0.0270 (7)	0.0243 (7)	0.0276 (7)	−0.0007 (5)	0.0098 (5)	−0.0017 (5)
C11A	0.0246 (8)	0.0192 (7)	0.0260 (8)	−0.0050 (6)	0.0027 (6)	0.0011 (6)
C12	0.0206 (6)	0.0195 (6)	0.0196 (6)	−0.0022 (5)	−0.0021 (5)	0.0011 (4)
C13	0.0208 (6)	0.0183 (6)	0.0172 (5)	0.0008 (5)	−0.0034 (4)	−0.0006 (4)
C14	0.0236 (6)	0.0166 (6)	0.0172 (5)	−0.0002 (5)	−0.0030 (5)	0.0007 (4)

Geometric parameters (Å, º)

I1—C13	2.0929 (15)	C6—C7	1.489 (2)
F1—C12	1.346 (2)	C6—H6A	0.9800
F2—C14	1.3446 (19)	C6—H6B	0.9800
O1—C2	1.306 (2)	C6—H6C	0.9800
O1—H1	0.903 (18)	C7—C8	1.396 (2)
O2—C4	1.275 (2)	C8—C9	1.404 (2)
N1—C7	1.341 (2)	C9—C10	1.487 (2)
N1—N2	1.3516 (19)	C10—H10A	0.9800
N1—C11B	1.48 (2)	C10—H10B	0.9800
N1—H1NA	0.891 (17)	C10—H10C	0.9800
N2—C9	1.341 (2)	O3A—H1OA	0.870 (18)
N2—C11A	1.474 (2)	O3A—H2OA	0.863 (18)
N2—H1NB	0.8501 (13)	C11A—H11A	0.9800
C1—C2	1.494 (3)	C11A—H11B	0.9800
C1—H1A	0.9800	C11A—H11C	0.9800
C1—H1B	0.9800	O3B—H1OB	0.8500
C1—H1C	0.9800	O3B—H2OB	0.8500
C2—C3	1.396 (2)	C11B—H11D	0.9800
C3—C4	1.430 (2)	C11B—H11E	0.9800
C3—C8	1.480 (2)	C11B—H11F	0.9800
C4—C5	1.493 (3)	C12—C14^{i}	1.386 (2)
C5—H5A	0.9800	C12—C13	1.389 (2)
C5—H5B	0.9800	C13—C14	1.383 (2)
C5—H5C	0.9800		

C2—O1—H1	102 (2)	N1—C7—C8	107.67 (14)
C7—N1—N2	109.55 (13)	N1—C7—C6	121.26 (14)
C7—N1—C11B	126.3 (9)	C8—C7—C6	131.05 (15)
N2—N1—C11B	122.8 (9)	C7—C8—C9	106.04 (13)
C7—N1—H1NA	132 (2)	C7—C8—C3	126.71 (14)
N2—N1—H1NA	118 (2)	C9—C8—C3	127.23 (14)
C9—N2—N1	108.99 (13)	N2—C9—C8	107.74 (13)
C9—N2—C11A	130.98 (14)	N2—C9—C10	123.13 (15)

N1—N2—C11A	119.95 (13)	C8—C9—C10	129.12 (14)
C9—N2—H1NB	137.18 (15)	C9—C10—H10A	109.5
N1—N2—H1NB	113.79 (13)	C9—C10—H10B	109.5
C2—C1—H1A	109.5	H10A—C10—H10B	109.5
C2—C1—H1B	109.5	C9—C10—H10C	109.5
H1A—C1—H1B	109.5	H10A—C10—H10C	109.5
C2—C1—H1C	109.5	H10B—C10—H10C	109.5
H1A—C1—H1C	109.5	H1OA—O3A—H2OA	99 (3)
H1B—C1—H1C	109.5	N2—C11A—H11A	109.5
O1—C2—C3	121.87 (18)	N2—C11A—H11B	109.5
O1—C2—C1	115.20 (17)	H11A—C11A—H11B	109.5
C3—C2—C1	122.93 (16)	N2—C11A—H11C	109.5
C2—C3—C4	118.41 (16)	H11A—C11A—H11C	109.5
C2—C3—C8	120.48 (15)	H11B—C11A—H11C	109.5
C4—C3—C8	121.11 (15)	H1OB—O3B—H2OB	124.5
O2—C4—C3	120.93 (18)	N1—C11B—H11D	109.5
O2—C4—C5	117.64 (17)	N1—C11B—H11E	109.5
C3—C4—C5	121.42 (16)	H11D—C11B—H11E	109.5
C4—C5—H5A	109.5	N1—C11B—H11F	109.5
C4—C5—H5B	109.5	H11D—C11B—H11F	109.5
H5A—C5—H5B	109.5	H11E—C11B—H11F	109.5
C4—C5—H5C	109.5	F1—C12—C14^{i}	118.30 (14)
H5A—C5—H5C	109.5	F1—C12—C13	120.07 (14)
H5B—C5—H5C	109.5	C14^{i}—C12—C13	121.63 (15)
C7—C6—H6A	109.5	C14—C13—C12	117.26 (14)
C7—C6—H6B	109.5	C14—C13—I1	122.36 (11)
H6A—C6—H6B	109.5	C12—C13—I1	120.38 (12)
C7—C6—H6C	109.5	F2—C14—C13	120.58 (14)
H6A—C6—H6C	109.5	F2—C14—C12^{i}	118.32 (15)
H6B—C6—H6C	109.5	C13—C14—C12^{i}	121.11 (14)

Symmetry code: (i) −*x*+1, −*y*+1, −*z*.

Hydrogen-bond geometry (Å, º)

D—H···*A*	*D*—H	H···*A*	*D*···*A*	*D*—H···*A*
O1—H1···O2	0.90 (2)	1.59 (2)	2.456 (3)	159 (3)
O3*A*$^{a—H1OA}$a···Br1	0.87 (2)	2.44 (2)	3.2843 (16)	165 (3)
O3*A*$^{a—H2OA}$a···Br1^{ii}	0.86 (2)	2.44 (2)	3.2667 (16)	161 (3)
N1—H1*NA*$^{a···O3A}$a	0.89 (2)	1.75 (2)	2.641 (2)	174 (3)
O3*B*$^{b—H1OB}$b···Br1^{iii}	0.85	2.47	3.317 (15)	180
O3*B*$^{b—H2OB}$b···Br1^{ii}	0.85	2.56	3.406 (15)	180
N2—H1*NB*$^{b···O3B}$b	0.85 (1)	1.78 (2)	2.628 (15)	180 (1)

Symmetry codes: (ii) −*x*+2, *y*+1/2, −*z*+1/2; (iii) *x*, −*y*+3/2, *z*+1/2.